PHYSICAL REVIEW D **75,** 054029 (2007)

Charm parton content of the nucleon

J. Pumplin,[1,*] H. L. Lai,[1,2,3] and W. K. Tung[1,2]
[1]*Michigan State University, E. Lansing, Michigan, USA*
[2]*University of Washington, Seattle, Washington, USA*
[3]*Taipei Municipal University of Education, Taipei, Taiwan*
(Received 9 February 2007; published 26 March 2007)

We investigate the charm sector of the nucleon structure phenomenologically, using the most up-to-date global QCD analysis. Going beyond the common assumption of purely radiatively generated charm, we explore possible degrees of freedom in the parton parameter space associated with nonperturbative (intrinsic) charm in the nucleon. Specifically, we explore the limits that can be placed on the intrinsic charm (IC) component, using all relevant hard-scattering data, according to scenarios in which the IC has a form predicted by light-cone wave function models; or a form similar to the light sea-quark distributions. We find that the range of IC is constrained to be from zero (no IC) to a level 2–3 times larger than previous model estimates. The behaviors of typical charm distributions within this range are described, and their implications for hadron collider phenomenology are briefly discussed.

DOI: 10.1103/PhysRevD.75.054029 PACS numbers: 12.38.Qk, 12.38.Bx, 13.60.Hb, 13.85.Qk

I. INTRODUCTION

The parton distribution functions (PDFs) that describe the quark and gluon structure of the nucleon at short distances are essential inputs to the calculation of all high energy processes at hadron colliders. They are therefore important for carrying out searches for new physics, as well as for making precision tests of the standard model (SM), in regions where perturbative quantum chromodynamics (PQCD) theory is applicable. Although much progress has been made in the last 20 years in determining the PDFs by global QCD analysis of a wide range of hard processes, very little is known phenomenologically about the heavy quark (charm c and bottom b) and antiquark ($\bar{c}$, $\bar{b}$) content of the nucleon [1,2].

Knowledge of the heavy quark components is inherently important as an aspect of the fundamental structure of the nucleon. In addition, the heavy quarks are expected to play an increasingly significant role in the physics programs of the Tevatron Run II and the Large Hadron Collider (LHC), since many new processes of interest, such as single-top production and Higgs production in the SM and beyond, are quite sensitive to the heavy quark content of the nucleon.

Existing global QCD analyses extract the PDFs by comparing a wide range of hard-scattering data to perturbative QCD theory. In these analyses, one usually adopts the ansatz that heavy quark partons in the nucleon are "radiatively generated," i.e., they originate only from QCD evolution, starting from a null distribution at a factorization scale of approximately the relevant quark mass. This is motivated, on the theoretical side, by the notion that heavy quark degrees of freedom should be perturbatively calculable; and on the practical side, by the lack of clearly identifiable experimental constraints on these degrees of freedom in existing data. Neither of those considerations justifies the ansatz, however—especially for charm, whose mass lies in between the soft and hard energy scales. In fact, many nonperturbative models, particularly those based on the light-cone wave function picture, expect an "intrinsic charm" (IC) component of the nucleon at an energy scale comparable to m_c, the mass of the charm quark. This IC component, if present at a low energy scale, will participate fully in QCD dynamics and evolve along with the other partons as the energy scale increases. It can therefore have observable consequences on physically interesting processes at high energies and short distances.

With recent advances in the implementation of the general perturbative QCD formalism to incorporate heavy quark mass effects [3,4], and the availability of comprehensive precision data from HERA, the Tevatron, and fixed-target experiments, we are now in a position to study the charm content of the nucleon phenomenologically, with minimal model-dependent assumptions. This paper represents a first systematic effort to perform this study and answer the following questions: (i) do current theory and experiment determine, or place useful limits on, the charm component of the nucleon at the scale of m_c; (ii) if a nonvanishing charm distribution is allowed, can current global QCD analysis distinguish its shape between a form typical of light sea quarks (peaked at small x) and the form predicted in light-cone wave function models (concentrated at moderate and large x); and (iii) what are the implications of IC for the Tevatron and the LHC physics programs?

II. CHARM PARTONS AT THE SCALE $\mu_0 \approx m_c$

Let $f_a(x, \mu)$ denote the PDF of parton flavor a inside the proton at momentum fraction x and factorization scale μ.

*Electronic address: pumplin@pa.msu.edu

At short distances, corresponding to large μ, the scale-dependence of $f_a(x, \mu)$ is governed by the QCD evolution equation, with perturbatively calculable evolution kernals (splitting functions). Thus, the set of PDFs $\{f_a(x, \mu)\}$ are fully determined once their functional form in x is specified at a fixed scale $\mu = \mu_0$, provided μ_0 is large enough to be in the region where PQCD applies. In practice, μ_0 is usually chosen to be on the order 1–2 GeV, which is at the borderline between the short-distance (perturbative) and long-distance (nonperturbative) regions. For the gluon and the light quarks ($a = g, u, d, s$), the $f_a(x, \mu_0)$ are certainly nonperturbative in origin. They must be determined phenomenologically through global QCD analysis that compares the theoretical predictions with a wide range of experimental data on hard processes [4–6]. In the case of charm and bottom quarks, we need to examine the situation more closely. In this paper, we shall focus, in particular, on charm. For convenience, we use the shorthand notation $c(x, \mu) \equiv f_c(x, \mu)$, and frequently omit the argument μ, i.e., use $c(x)$ in place of $c(x, \mu)$.

Over the energy range of most interest to current high energy physics, the charm quark behaves as a parton, and is characterized by a PDF $c(x, \mu)$ that is defined for $\mu \geq m_c$. It is common in global QCD analysis to consider charm a *heavy quark*, and to adopt the ansatz $c(x, \mu_0 = m_c) = 0$ as the initial condition for calculating $c(x, \mu)$ at higher energy scales by QCD evolution. This is the so-called *radiatively generated charm* scenario. In the context of global analysis, this ansatz implies that the charm parton does not have any independent degrees of freedom in the parton parameter space: $c(x, \mu)$ is completely determined by the gluon and light-quark parton parameters.

However, nature does not have to subscribe to this scenario. First, although m_c (~ 1.3 GeV) is larger than $\Lambda_{\rm QCD}$ (~ 0.2–0.4 GeV, depending on the number of effective flavors), it is actually of the same order of magnitude as the nucleon mass, which must certainly be considered as being of a nonperturbative scale. Second, the ansatz itself is ill-defined, since: (i) the initial condition $c(x, \mu_0) = 0$ depends sensitively on the choice of μ_0; and (ii) PQCD only suggests that μ_0 be of the same order of magnitude as m_c, but does not dictate any particular choice. Since the μ-dependence of $c(x, \mu)$ is relatively steep in the threshold region, the condition $c(x, \mu_0) = 0$ for a given choice of μ_0 is physically quite different from that at a different choice of μ_0. Third, many nonperturbative models give nonzero predictions for $c(x, \mu_0)$—again, for unspecified $\mu_0 \sim m_c$ [7–9]. We therefore wish to study the nucleon structure in a formalism that allows for nonperturbative charm.

To carry out a systematic study of the charm sector of nucleon structure, one needs: (i) a general global analysis framework that includes a coherent treatment of nonzero quark masses in PQCD; and (ii) comprehensive experimental inputs that have the potential to constrain the charm degrees of freedom. (Earlier efforts [10,11] treated light partons and the IC component as dynamically uncoupled, and were done outside the framework of a global analysis.) Recent advances on both fronts make this study now possible. In the following, we extend the recent CTEQ6.5 global analysis [4,12] to include a charm sector with its own independent degrees of freedom at the initial factorization scale $\mu_0 = m_c$. We shall address the questions posed in the introduction by examining the results of global analyses performed under three representative scenarios.

The first two scenarios invoke the light-cone Fock space picture [13] of nucleon structure. In this picture, IC appears mainly at large momentum fraction x, because states containing heavy quarks are suppressed according to their off-shell distance, which is proportional to $(p_\perp^2 + m^2)/x$. Hence components with large mass m appear preferentially at large x. It has recently been shown that indeed a wide variety of light-cone models all predict similar shapes in x [9].

The specific light-cone models we take as examples are the original model of Brodsky *et al.* [7] (BHPS), and a model in which the intrinsic charm arises from virtual low-mass meson + baryon components such as $\bar{D}^0\Lambda_c^+$ of the proton—a "meson-cloud" picture [14–16]. It has been shown that these two models reasonably represent other natural choices in the light-cone picture [9]. They are fairly similar to each other as well; but the meson-cloud model also predicts a difference between $c(x)$ and $\bar{c}(x)$, so it provides an estimate of the size of possible charm/anti-charm differences.

The light-cone formalism is not developed to a point where the normalization of $uudc\bar{c}$ or $uudb\bar{b}$ components can be calculated with any confidence [9]—though estimates on the order of 1% have been proposed in several studies [14,17,18]. In our phenomenological approach, it is appropriate to treat the magnitude of IC as a quantity to be determined by comparison with data.

The x-dependence predicted by the BHPS model [7] is

$$c(x) = \bar{c}(x) = Ax^2[6x(1+x)\ln x + (1-x)(1+10x+x^2)]. \quad (1)$$

We use this form at scale $\mu_0 = m_c$ for the BHPS scenario. The normalization constant A that controls the magnitude of IC in this model is treated as a variable parameter in our study. The magnitude of IC can be conveniently characterized by the momentum fraction carried by $c + \bar{c}$—see Eq. (4).

The exact x-dependence predicted by the meson-cloud model cannot be given by a simple formula, since it involves convolutions of the charmed meson and baryon distributions in the proton with the quark distributions within the meson and baryon. However, it was shown in Ref. [9] that the charm distributions in this model can be very well approximated by

$$c(x) = Ax^{1.897}(1-x)^{6.095}, \quad (2)$$

$$\bar{c}(x) = \bar{A}x^{2.511}(1-x)^{4.929}, \quad (3)$$

where the normalization constants A and $\bar{A}$ are determined by the requirement of the quark number sum rule $\int_0^1[c(x) - \bar{c}(x)]dx = 0$, which specifies $A/\bar{A}$; and the overall magnitude of IC that is to be varied in our study.

In contrast to these light-cone scenarios, we also examine a purely phenomenological scenario in which the shape of the charm distribution is *sealike*—i.e., similar to that of the light flavor sea quarks, except for an overall mass-suppression. In this scenario, for simplicity, we assume $c(x) = \bar{c}(x) \propto \bar{d}(x) + \bar{u}(x)$ at the starting scale $\mu_0 = m_c$.

In each of the three scenarios, the initial nonperturbative $c(x)$ and $\bar{c}(x)$ specified above is used as input to the general-mass perturbative QCD evolution framework discussed in detail in [4]. We then determine the range of magnitudes for IC that is consistent with our standard global analysis fit to data. This is described in the next section.

III. GLOBAL QCD ANALYSIS WITH INTRINSIC CHARM

For these global fits, we use the same theoretical framework and experimental input data sets that were used for the recent CTEQ6.5 analysis [4], which made the traditional ansatz of no IC. Notable improvements over previous CTEQ global analyses [5] are: (i) the theory includes a comprehensive treatment of quark mass effects in DIS according to the PQCD formalism of Collins [19]; and (ii) the full HERA I data on neutral current and charged current total inclusive cross sections, as well as heavy quark production cross sections, are incorporated. Published correlated systematic errors are used wherever they are available. Fixed-target DIS, Drell-Yan, and hadron collider data that were used previously are also included [4,5].

For each model of IC described in Sec. II, we carry out a series of global fits with varying magnitudes of the IC component. From the results, we infer the ranges of the amount of IC allowed by current data within each scenario.

It is natural to characterize the magnitude of IC by the momentum fraction $\langle x\rangle_{c+\bar{c}}$ carried by charm at our starting scale for evolution $\mu = 1.3$ GeV. This is just the first moment of the $c + \bar{c}$ momentum distribution:

$$\langle x\rangle_{c+\bar{c}} = \int_0^1 x[c(x) + \bar{c}(x)]dx. \quad (4)$$

(In the context of light-cone models, the zeroth moment $\int_0^1 c(x)dx = \int_0^1 \bar{c}(x)dx$ (= total number of charm pairs) is often used to characterize the magnitude of IC. In more general cases, it is not a good measure of IC because it is overly sensitive to the small-x behavior. In particular, this integral does not even converge if $c(x)$ has the same power-law behavior as light quarks in the limit $x \to 0$, as in our sealike model.)

The quality of each global fit is measured by χ^2_{global}, supplemented by considerations of the goodness-of-fit to the individual experiments included in the fit. (The procedure has been fully described in Ref. [4,5].) The three curves in Fig. 1 show χ^2_{global} as a function of $\langle x\rangle_{c+\bar{c}}$ for the three models under consideration.

We observe first that in the lower range, $0 < \langle x\rangle_{c+\bar{c}} \sim 0.01$, χ^2_{global} varies very little, i.e., the quality of the fit is very insensitive to $\langle x\rangle_{c+\bar{c}}$ in this interval. This means that *the global analysis of hard-scattering data provides no evidence either for or against IC up to* $\langle x\rangle_{c+\bar{c}} \sim 0.01$.

Beyond $\langle x\rangle_{c+\bar{c}} \sim 0.01$, all three curves in Fig. 1 rise steeply with $\langle x\rangle_{c+\bar{c}}$—global fits do place useful upper bounds on IC. The upper dots along the three curves represent marginal fits in each respective scenario, beyond which the quality of the fit becomes unacceptable according to the procedure established in Refs. [4,5]—one or more of the individual experiments in the global fit is no longer fitted within the 90% confidence level. (There is no particular data set that can be identified as particularly sensitive to IC—the limiting feature is generally one of the high-precision large-statistics DIS experiments from HERA.) This implies that *the global QCD analysis rules out the possibility of an IC component much larger than* 0.02 *in momentum fraction*.

We note that the allowed range for $\langle x\rangle_{c+\bar{c}}$ is somewhat wider for the sealike IC model. This is understandable,

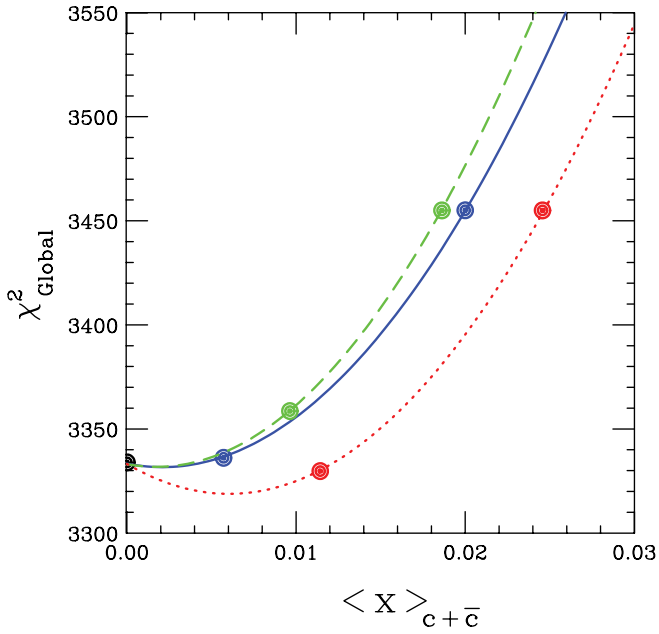

FIG. 1 (color online). Goodness-of-fit vs momentum fraction of IC at the starting scale $\mu = 1.3$ GeV for three models of IC: BHPS (solid curve); meson cloud (dashed curve); and sealike (dotted curve). Large dots indicate the specific fits that are shown in Figs. 2–4.

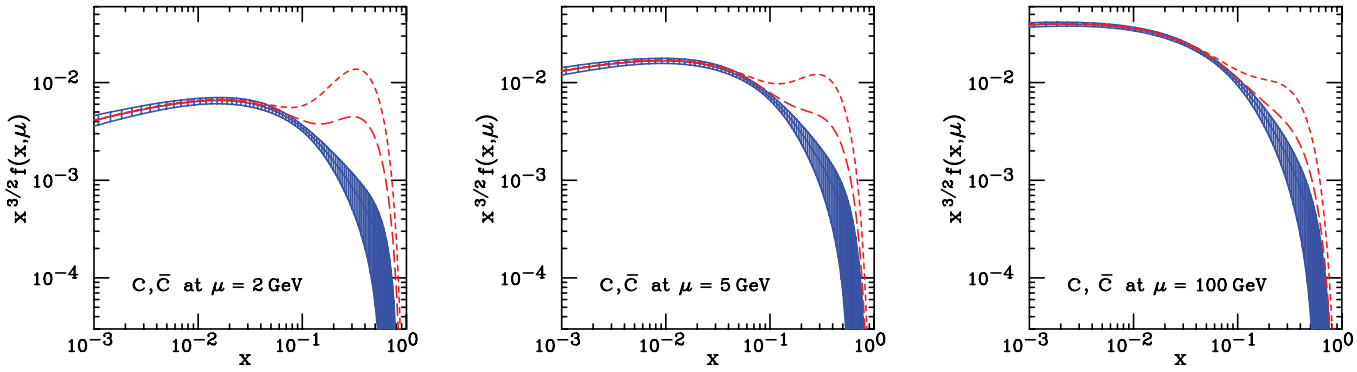

FIG. 2 (color online). Charm quark distributions from the BHPS IC model. The three panels correspond to scales $\mu = 2$, $\mu = 5$, and $\mu = 100$ GeV. The long-dashed (short-dashed) curve corresponds to $\langle x \rangle_{c+\bar{c}} = 0.57\%$ (2.0%). The solid curve and shaded region show the central value and uncertainty from CTEQ6.5, which contains no IC.

because under this scenario, the charm component is more easily interchangeable with the other sea-quark components, in its contribution to the inclusive cross sections that are used in the analysis; whereas the hard c and $\bar{c}$ components of the light-cone models are not easily mimicked by other sea quarks.

The PDF sets that correspond to the three limiting cases (upper dots), along with three lower ones on the same curves that represent typical, more moderate, model candidates (lower dots), will be explored in detail next.

BHPS model results: Fig. 2 shows the charm distributions $c(x) = \bar{c}(x)$ at three factorization scales that arise from the BHPS model, along with results from the CTEQ6.5 PDFs which have no IC.

The short-dash curves correspond to the marginally allowed amount of IC ($\langle x \rangle_{c+\bar{c}} = 0.020$) indicated by the upper dot on the BHPS curve in Fig. 1. The long-dash curves correspond to IC that is weaker by a factor of ~ 3, indicated by the lower dot ($\langle x \rangle_{c+\bar{c}} = 0.0057$) on the BHPS curve in Fig. 1. This point corresponds to the traditional estimate of 1% IC probability in the BHPS model, i.e., $\int_0^1 c(x)dx = \int_0^1 \bar{c}(x)dx = 0.01$, at the starting scale $\mu_0 = 1.3$ GeV. This physically motivated light-cone model estimate thus lies *well within the phenomenological bounds set by our global analysis*.

We see that at low factorization scales, this model produces a peak in the charm distribution at $x \approx 0.3$. This peak survives in the form of a shoulder even at a scale as large as $\mu = 100$ GeV. At that scale, IC strongly increases $c(x)$ and $\bar{c}(x)$ above the gluon splitting contribution at $x > 0.1$, while making a negligible contribution at $x < 0.1$.

Meson-cloud model results: Fig. 3 shows the charm distributions that arise from the $D_0 \Lambda_c^+$ meson-cloud model, together with the results from CTEQ6.5 which has no IC. In the meson-cloud model, the charm ($c(x)$) and anticharm ($\bar{c}(x)$) distributions are different.

The short-dash (short-dashed-dotted) curves correspond to the maximum amount of IC $c(x)$ ($\bar{c}(x)$) that is allowed by the data ($\langle x \rangle_{c+\bar{c}} = 0.018$), while the long-dash (long-dash-dot) curves show a smaller amount ($\langle x \rangle_{c+\bar{c}} = 0.0096$), and the shaded region shows CTEQ6.5 which has no IC. Again we see that IC can substantially increase the charm PDFs at $x > 0.1$, even at a large factorization scale.

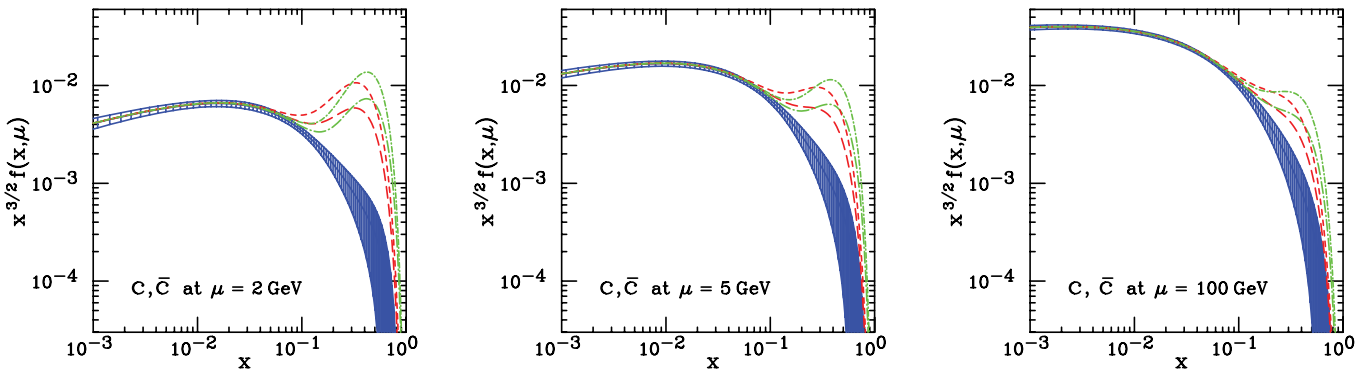

FIG. 3 (color online). Same as Fig. 2, except for the meson-cloud model. The long-dash (short-dashed) curves correspond to $\langle x \rangle_{c+\bar{c}} = 0.96\%$ (1.9%).

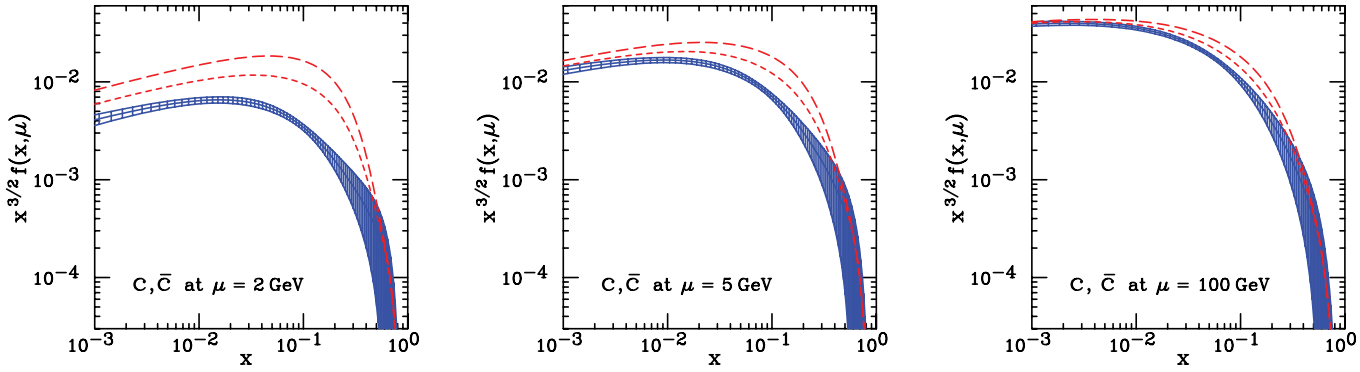

FIG. 4 (color online). Same as Fig. 2, but for the sealike scenario. The long-dashed (short-dashed) curves correspond to $\langle x \rangle_{c+\bar{c}} = 2.4\%$ (1.1%).

The difference between c and $\bar{c}$ due to IC is seen to be potentially quite large. The sign of the difference is such that $\bar{c}(x) > c(x)$ for $x \to 1$, as explained in Ref. [9]. Experimental evidence for $c(x) \neq \bar{c}(x)$ may be difficult to obtain; but it is worth considering because it would provide an important constraint on the nonperturbative physics—as well as supplying a direct proof of intrinsic charm, since $c\bar{c}$ pairs produced by gluon splitting are symmetric to NLO. (QCD evolution at NNLO can produce $c(x) \neq \bar{c}(x)$ from the valence $u(x) \neq \bar{u}(x)$ and $d(x) \neq \bar{d}(x)$, but the predicted asymmetry is only a few percent [20].)

Sealike model results: Fig. 4 shows the charm distributions that arise from a model in which IC is assumed to have the same shape in x as the light-quark sea $\bar{u}(x) + \bar{d}(x)$ at the starting scale $\mu_0 = 1.3$ GeV. The long-dash curve again corresponds to the maximum amount of IC of this type that is allowed by the data ($\langle x \rangle_{c+\bar{c}} = 0.024$), while the short-dash curve shows an intermediate amount ($\langle x \rangle_{c+\bar{c}} = 0.011$), and the shaded region shows CTEQ6.5 which has no IC.

We see that IC in this sealike form can increase the charm PDFs over a rather large region of moderate x. As a result, it may have important phenomenological consequences for hard processes that are initiated by charm.

IV. COMPARISON WITH LIGHT PARTONS

In this section, we compare the charm content of the nucleon with the other flavors at various hardness scales. Figure 5 shows the charm distribution with no IC, or IC with shape given by the BHPS model with the two strengths discussed previously, compared to gluon, light quark, and light antiquark distributions from the CTEQ6.5 best fit. By comparing the three panels of this figure, one can recognize the standard characteristics of DGLAP evolution: at increasing scale, the PDFs grow larger at small x and smaller at large x; while the differences between q and $\bar{q}$, and the differences between flavors, all get smaller.

This figure shows that the light-cone form for IC has negligible effects for $x < 0.05$, while it can make $c(x)$ and $\bar{c}(x)$ larger than any of $\bar{u}(x)$, $\bar{d}(x)$, $s(x)$, and $\bar{s}(x)$ for $x > 0.2$. Similar results hold for the meson-cloud model (not shown), since the essential basis is the large-x behavior that is characteristic of the light-cone picture.

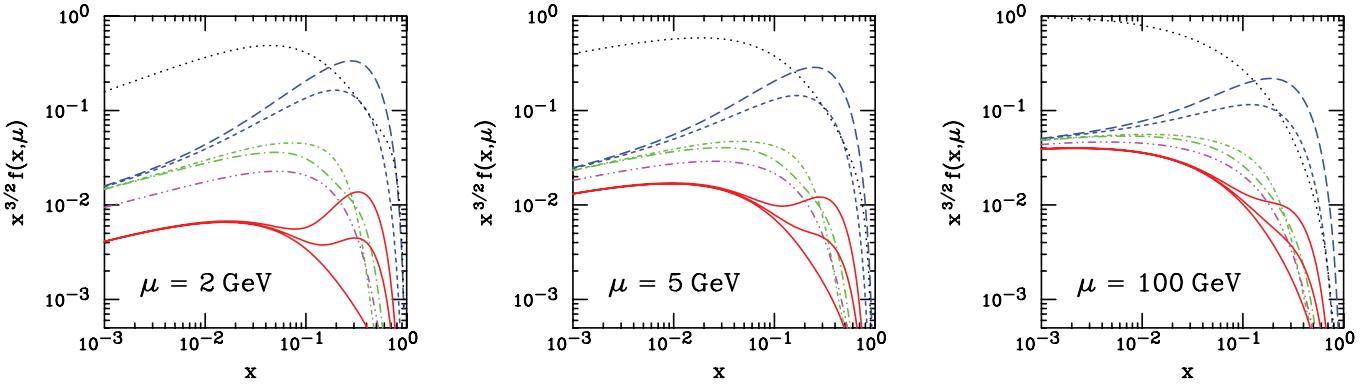

FIG. 5 (color online). Comparison of charm with other flavors: u, $\bar{u}$ (long-dash, long-dash-dotted); d, $\bar{d}$ (short-dashed, short-dashed-dotted); $s = \bar{s}$ (dashed-dot-dotted), g (dotted). The solid curves are $c = \bar{c}$ with no IC (lowest) or the two magnitudes of IC in the BHPS model that are discussed in the text.

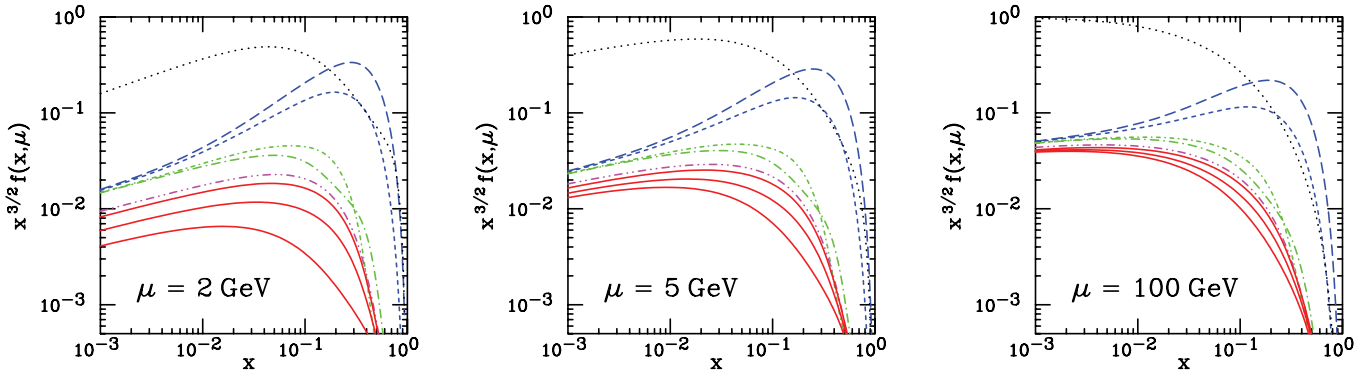

FIG. 6 (color online). Same as Fig. 5, but for sealike IC.

Figure 6 similarly shows the charm content for the scenarios of no IC, or IC with a "sealike" shape for the two normalizations discussed previously. In this case, unlike the light-cone forms, charm remains smaller than the other sea quarks, including s and $\bar{s}$, at all values of x. However, this figure shows that IC can raise the c and $\bar{c}$ distributions by up to a factor of $\sim$2 above their traditional radiative-only estimates, so it can have an important effect on processes that are initiated by charm.

Figs. 5 and 6 also show that in every scenario, $c(x)$ and $\bar{c}(x)$ remain small compared to u, d, and g.

V. THE CHARM DISTRIBUTION AT VARIOUS ENERGY SCALES

The effect of evolution of the charm distributions in each scenario can be seen by comparing the three panels within each of Figs. 2–4. But to show the evolution in more detail, we plot the x-dependence at scales $\mu = 1.3$, 2.0, 3.16, 5, 20, 100 GeV together on the same figure. In place of the logarithmic scale in x, we use a scale that is linear in $x^{1/3}$ in order to display the important large-x region more clearly.

The left panel of Fig. 7 has no IC; the center panel is the BHPS model (maximal level); and the right panel is the sealike IC model (maximal level). In all cases, as the scale increases, the charm distribution becomes increasingly soft as the result of QCD evolution. As one would expect, the IC component dominates at low energy scales. The radiatively generated component (coming mainly from gluon splitting) increases rapidly in importance with increasing scale. A two-component structure appears in these plots at intermediate scales, say $\mu = 5$ GeV, where IC is dominant at large x and radiatively generated is dominant at small x. As noted previously, even at a rather high energy scale of $\mu = 100$ GeV the IC component is still very much noticeable in the light-cone wave function models. In all cases, the intrinsic component is quite large in magnitude compared to the purely radiatively generated case in the region, say, $x > 0.1$. Thus, the existence of IC would have observable consequences in physical processes at future hadron colliders that depend on the charm PDF in this kinematic region.

VI. SUMMARY AND IMPLICATIONS

As a natural extension of the CTEQ6.5 global analysis [4,12], we have determined the range of magnitudes for intrinsic charm that is consistent with an up-to-date global

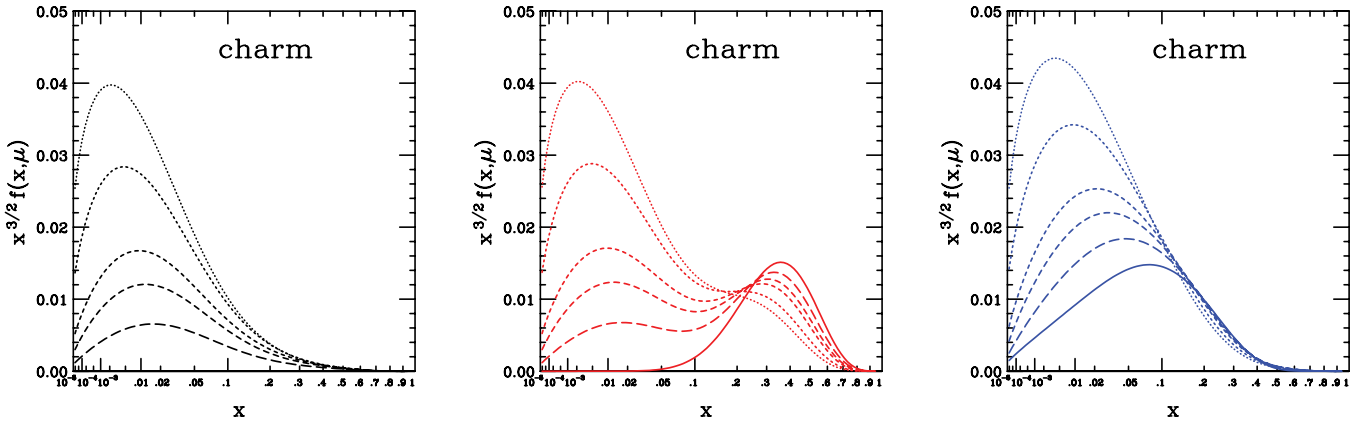

FIG. 7 (color online). Charm distributions at scale $\mu = 1.3$ (solid), 2.0, 3.16, 5, 20, 100 GeV (dotted). Left: no IC; center: BHPS model with maximal IC consistent with experiment; right: sealike model with maximal IC consistent with experiment.

QCD analysis of hard-scattering data, for various plausible assumptions on the shape of the x-distribution of IC at a low factorization scale.

For shapes suggested by light-cone models, we find that the global analysis is consistent with anywhere from zero IC up to ~3 times the amount that has been estimated in more model-dependent studies. In these models, there can be a large enhancement of $c(x)$ and $\bar{c}(x)$ at $x > 0.1$, relative to previous PDF analyses which assume no IC. The enhancement persists to scales as large as $\mu \sim 100$ GeV, and can therefore have an important influence on charm-initiated processes at the Tevatron and LHC. Large differences between $c(x)$ and $\bar{c}(x)$ for $x > 0.1$ are also natural in some models of this type.

For an assumed shape of IC similar to other sea quarks at low factorization scale, there can also be a significant enhancement of $c(x)$ and $\bar{c}(x)$ relative to traditional no-IC analyses. In this case, the enhancement is spread more broadly in x, roughly over the region $0.01 < x < 0.50$.

What experimental data could be used to pin down the intrinsic charm contribution? An obvious candidate would be c and b production data from HERA; but these are already included in the analysis, and they do not have very much effect because the errors are rather large and because the data are mostly at small x where the dominant partonic subprocess is $\gamma g \to c\bar{c}$ rather than $\gamma c \to cX$. It may be possible to probe the subprocess $\gamma c \to cX$ more effectively by measuring specific angular differential distributions—see Ref. [21].

Future hadron collider measurements could place direct constraints on the charm PDF. For instance, in principle, the partonic process $g + c \to \gamma/Z + c$ is directly sensitive to the initial state charm distribution. The experimental signature would be Z plus a tagged charm jet in the final state. Such measurements would be experimentally very challenging, but potentially important [22,23]. The proposed future ep colliders eRHIC [24] and LHeC [25] would also be very helpful for the study of heavy quark parton distributions.

If IC is indeed present in the proton at a level on the order of what is allowed by the current data, it will have observable consequences in physical processes at future hadron colliders that depend on the charm PDF in the large x region. Interesting examples that have been proposed in the literature are: diffractive production of neutral Higgs bosons [26], and charged Higgs production at the LHC [27,28]. Application of our results to the latter process will be presented in Ref. [12].

The PDF sets with intrinsic charm that were used in this paper will be made available on the CTEQ webpage and via the LHAPDF standard, for use in predicting/analyzing experiments. They are designated by CTEQ6.5C.

ACKNOWLEDGMENTS

We thank Joey Huston, Pavel Nadolsky, Daniel Stump, and C.-P. Yuan for useful discussions. This work was supported in part by the U.S. National Science Foundation under Grant No. PHY-0354838, and by National Science Council of Taiwan under Grant No. 94(95)-2112-M-133-001.

[1] W. K. Tung, AIP Conf. Proc. **753**, 15 (2005).
[2] R. S. Thorne, hep-ph/0606307.
[3] R. S. Thorne, Phys. Rev. D **73**, 054019 (2006), and references therein.
[4] W. K. Tung, H. L. Lai, A. Belyaev, J. Pumplin, D. Stump, and C. P. Yuan, hep-ph/0611254.
[5] J. Pumplin, D. R. Stump, J. Huston, H. L. Lai, P. Nadolsky, and W. K. Tung, J. High Energy Phys. 07 (2002) 012; D. Stump, J. Huston, J. Pumplin, W. K. Tung, H. L. Lai, S. Kuhlmann, and J. F. Owens, J. High Energy Phys. 10 (2003) 046.
[6] R. S. Thorne, A. D. Martin, and W. J. Stirling, hep-ph/0606244, and references therein.
[7] S. J. Brodsky, P. Hoyer, C. Peterson, and N. Sakai, Phys. Lett. B **93**, 451 (1980).
[8] S. J. Brodsky, C. Peterson, and N. Sakai, Phys. Rev. D **23**, 2745 (1981); R. Vogt, Prog. Part. Nucl. Phys. **45**, S105 (2000); T. Gutierrez and R. Vogt, Nucl. Phys. **B539**, 189 (1999); G. Ingelman and M. Thunman, Z. Phys. C **73**, 505 (1997); J. Alwall, hep-ph/0508126.
[9] J. Pumplin, Phys. Rev. D **73**, 114015 (2006).
[10] B. W. Harris, J. Smith, and R. Vogt, Nucl. Phys. **B461**, 181 (1996).
[11] J. F. Gunion and R. Vogt, hep-ph/9706252.
[12] H. L. Lai, *et al.* (work in progress).
[13] S. J. Brodsky, hep-ph/0412101; S. J. Brodsky, Few Body Syst. **36**, 35 (2005).
[14] F. S. Navarra, M. Nielsen, C. A. A. Nunes, and M. Teixeira, Phys. Rev. D **54**, 842 (1996); S. Paiva, M. Nielsen, F. S. Navarra, F. O. Duraes, and L. L. Barz, Mod. Phys. Lett. A **13**, 2715 (1998).
[15] W. Melnitchouk and A. W. Thomas, Phys. Lett. B **414**, 134 (1997).
[16] F. M. Steffens, W. Melnitchouk, and A. W. Thomas, Eur. Phys. J. C **11**, 673 (1999).
[17] J. F. Donoghue and E. Golowich, Phys. Rev. D **15**, 3421 (1977).
[18] X. T. Song, Phys. Rev. D **65**, 114022 (2002).
[19] J. C. Collins and W. K. Tung, Nucl. Phys. **B278**, 934 (1986); J. C. Collins, Phys. Rev. D **58**, 094002 (1998).
[20] S. Catani, D. de Florian, G. Rodrigo, and W. Vogelsang, Phys. Rev. Lett. **93**, 152003 (2004).

[21] L. N. Ananikyan and N. Ya. Ivanov, hep-ph/0701076.
[22] TeV4LHC QCD Working Group, Nucl. Phys. **B762**, 256 (2007).
[23] P. Nadolsky *et al.* (unpublished).
[24] A. Deshpande, R. Milner, R. Venugopalan, and W. Vogelsang, Annu. Rev. Nucl. Part. Sci. **55**, 165 (2005); cf. also http://www.bnl.gov/eic.
[25] J. B. Dainton, M. Klein, P. Newman, E. Perez, and F. Willeke, hep-ex/0603016.
[26] S. J. Brodsky, B. Kopeliovich, I. Schmidt, and J. Soffer, Phys. Rev. D **73**, 113005 (2006).
[27] H. J. He and C. P. Yuan, Phys. Rev. Lett. **83**, 28 (1999); C. Balazs, H. J. He, and C. P. Yuan, Phys. Rev. D **60**, 114001 (1999).
[28] U. Aglietti *et al.*, hep-ph/0612172.